

Supplemental material

Chakrabarty et al., <https://doi.org/10.1083/jcb.201711022>

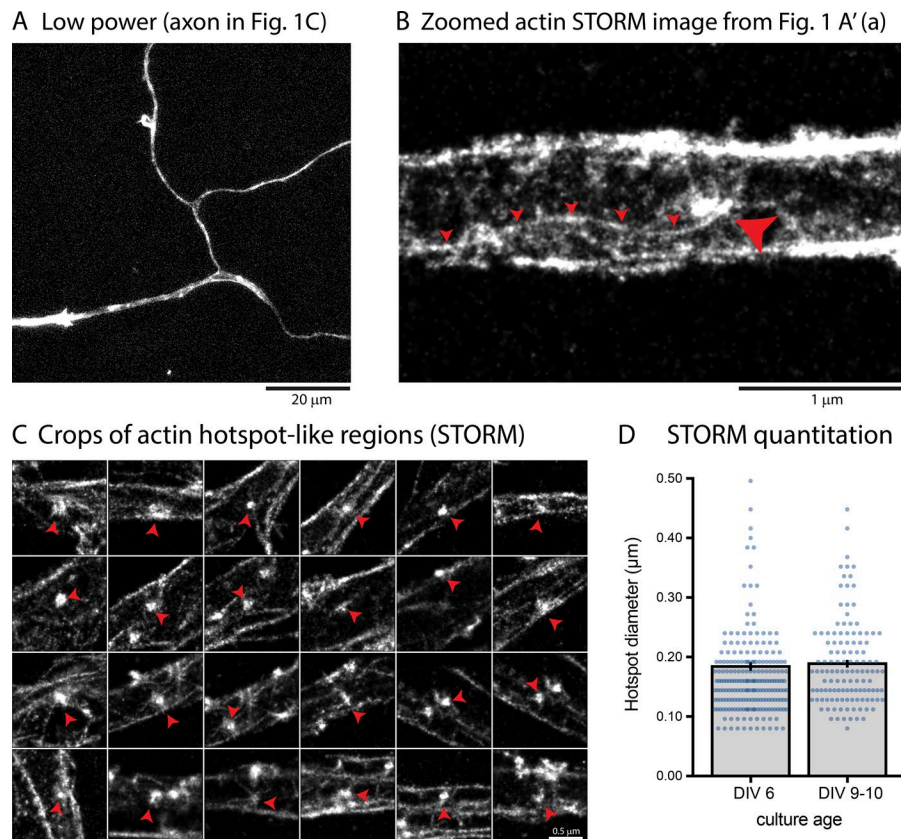


Figure S1. **Superresolution imaging of actin.** (A) Low-power image of axon shown in Fig. 1C. Note that the cell body is on left. (B) A higher magnification of the STORM image from Fig. 1 A' (a). Note the long filament (marked by small red arrowheads) that appears to emerge from the aster-like axonal actin cluster (large arrowhead). (C) Representative cropped phalloidin STORM images of hotspot-like clusters in axons (marked by arrowheads). (D) Quantification of the diameter of actin hotspot-like clusters in axons (from STORM images).

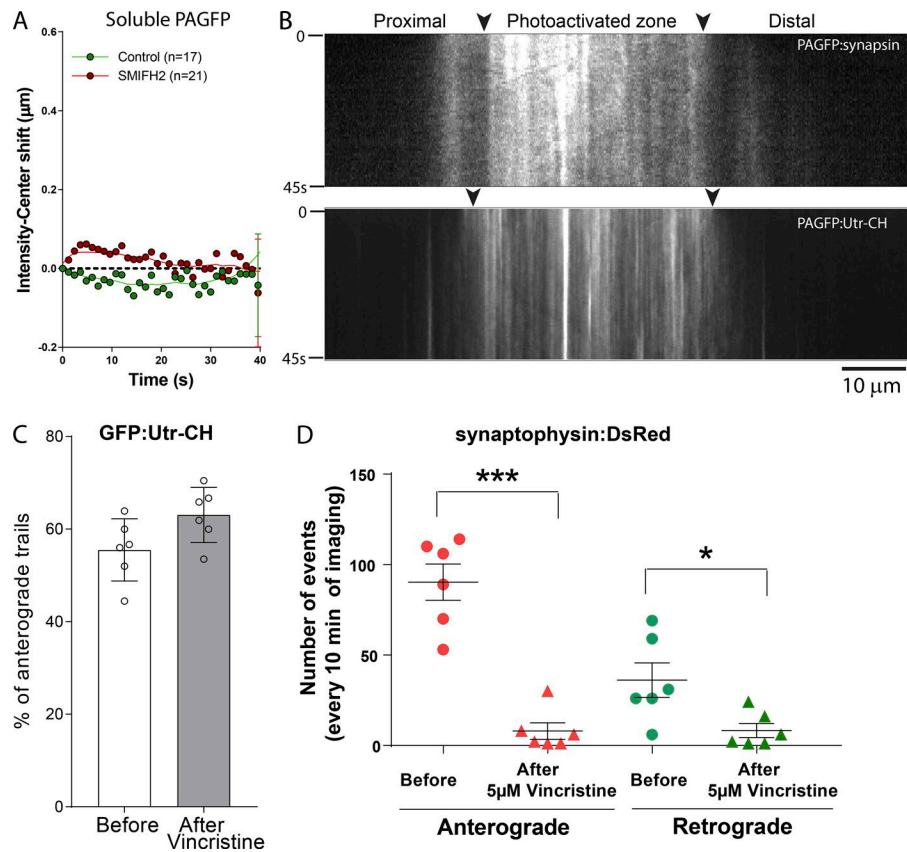


Figure S2. Axonal kinetics of soluble GFP and slow transport cargoes and effects of vincristine on vesicle trafficking. **(A)** Intensity center shifts of soluble untagged PAGFP and PAGFP:synapsin in control and formin inhibitor (SMIFH2)-treated axons. Curved lines are the smoothed fits of data. **(B)** Representative kymographs from axonal photoactivation of PAGFP:synapsin (top) and PAGFP:Utr-CH, two proteins conveyed in slow transport (bottom; elapsed time in seconds is shown on left). The photoactivated zone is marked by arrowheads, and elapsed time in seconds is shown on the left. **(C)** Effects of the MT-depolymerizing agent vincristine on actin trails. Note that vincristine treatment did not attenuate the anterograde bias in the actin trail frequency (Before, 55.5 ± 6.73 ; After, 63.06 ± 5.96). **(D)** As expected, vincristine led to a dramatic inhibition of vesicle transport as determined by synaptophysin imaging (*, $P < 0.05$; ***, $P < 0.001$, paired t test).

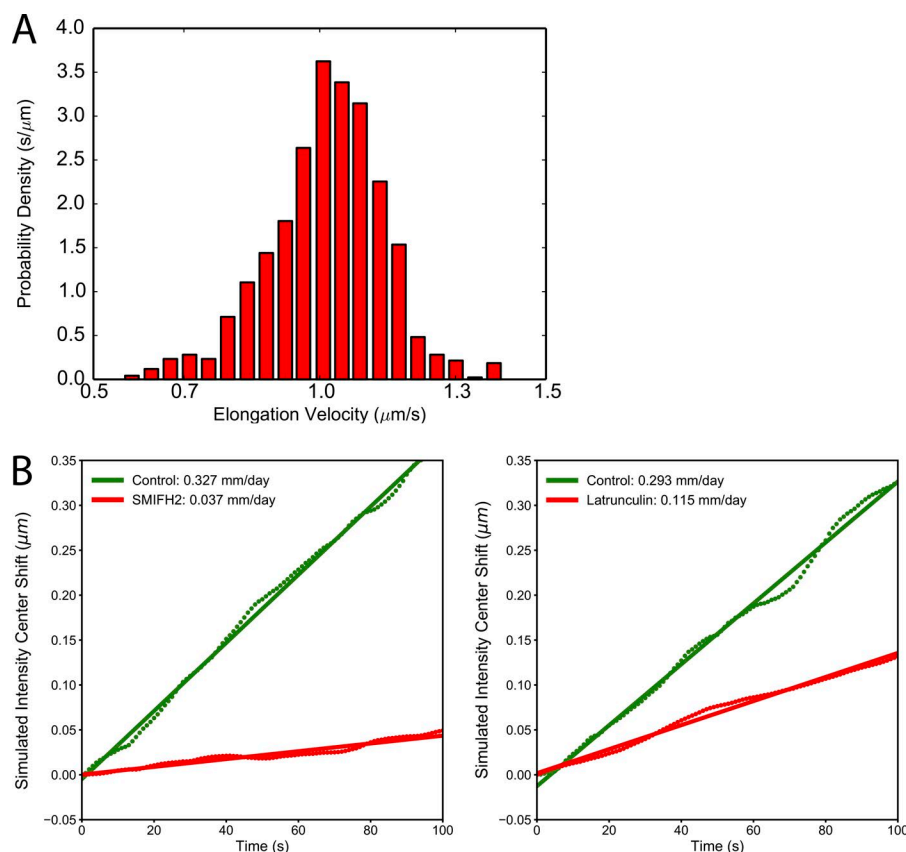
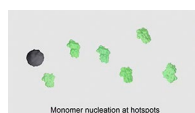
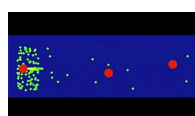


Figure S3. **Modeling of axonal actin.** (A) Distribution of actin trail elongation rates at a basal actin-monomer concentration of $47 \mu M$. The variability of the elongation velocities is due to variations in the lengths of individual trails as well as local variations in actin-monomer concentrations due to multiple trails continuously assembling and disassembling in the axon. (B) Simulation of transport rate of actin in the presence of latrunculin A (LatA) or SMIFH2 as described in Materials and methods (>500 independently seeded runs). Input values for these simulations were taken from before/after drug treatment experiments reported by Ganguly et al. (2015) (see Results and discussion for more details). Note the decrease in slow anterograde transport of actin after these treatments.



Video 1. **Animation of actin nucleation and elongation at hotspots.** The gray shape represents a hypothetical hotspot, and actin monomers (green) nucleate at hotspots with their barbed ends facing the hotspot. Note that as the filament elongates, individual actin monomers are translocated toward the growing (pointed) end.



Video 2. **Animation showing overall actin dynamics in axons and translocation of individual monomers.** Three virtual hotspots are shown (red circles) with actin monomers (green) nucleating at these regions. Note that free monomers are incorporated into the elongating filament (actin trail), with individual monomers facing the hotspots (not depicted here; see Video 1). Note left-to-right translocation of activated actin monomers (yellow) in the elongating actin trail. As the video plays, note disassembly of actin trails and subsequent incorporation of the resultant free monomers into new trails elongating on other hotspots.

Table S1 is a separate PDF showing parameters used in simulations

Reference

Ganguly, A., Y. Tang, L. Wang, K. Ladt, J. Loi, B. Dargent, C. Leterrier, and S. Roy. 2015. A dynamic formin-dependent deep F-actin network in axons. *J. Cell Biol.* 210:401–417. <https://doi.org/10.1083/jcb.201506110>